

# Phase transitions and equations of state of alkaline earth fluorides $\text{CaF}_2$ , $\text{SrF}_2$ , and $\text{BaF}_2$ to Mbar pressures

Susannah M. Dorfman,<sup>1</sup> Fuming Jiang,<sup>1,\*</sup> Zhu Mao,<sup>1,†</sup> Atsushi Kubo,<sup>1,‡</sup> Yue Meng,<sup>2</sup> Vitali B. Prakapenka,<sup>3</sup> and Thomas S. Duffy<sup>1</sup>

<sup>1</sup>*Department of Geosciences, Princeton University, Princeton, New Jersey 08544, USA*

<sup>2</sup>*High-Pressure Collaborative Access Team, Carnegie Institution of Washington, 9700 South Cass Avenue, Argonne, Illinois 60439, USA*

<sup>3</sup>*Consortium for Advanced Radiation Sources, University of Chicago, 9700 South Cass Avenue, Argonne, Illinois 60439, USA*

(Received 11 March 2010; revised manuscript received 28 April 2010; published 27 May 2010)

Phase transitions and equations of state of the alkaline earth fluorides  $\text{CaF}_2$ ,  $\text{SrF}_2$ , and  $\text{BaF}_2$  were examined by static compression to pressures as high as 146 GPa. Angle-dispersive x-ray diffraction experiments were performed on polycrystalline samples in the laser-heated diamond-anvil cell. We confirmed that at pressures less than 10 GPa all three materials undergo a phase transition from the cubic ( $Fm\bar{3}m$ ) fluorite structure to the orthorhombic ( $Pnam$ ) cotunnite-type structure. This work has characterized an additional phase transition in  $\text{CaF}_2$  and  $\text{SrF}_2$ : these materials were observed to transform to a hexagonal ( $P6_3/mmc$ )  $\text{Ni}_2\text{In}$ -type structure between 63–79 GPa and 28–29 GPa, respectively, upon laser heating. For  $\text{SrF}_2$ , the  $\text{Ni}_2\text{In}$ -type phase was confirmed by Rietveld refinement. Volumes were determined as a function of pressure for all high-pressure phases and fit to the third-order Birch-Murnaghan equation of state. For  $\text{CaF}_2$  and  $\text{SrF}_2$ , the fluorite-cotunnite transition results in a volume decrease of 8–10 %, while the bulk modulus of the cotunnite-type phase is the same or less than that of the fluorite phase within uncertainty. For all three fluorides, the volume reduction associated with the further transition to the  $\text{Ni}_2\text{In}$ -type phase is  $\sim 5\%$ . The percentage increase in the bulk modulus ( $\Delta K$ ) across the transition is greater when the cation is smaller. While for  $\text{BaF}_2$ ,  $\Delta K$  is 10–30 %,  $\Delta K$  values for  $\text{SrF}_2$  and  $\text{CaF}_2$  are 45–65 % and 20–40 %. Although shock data for  $\text{CaF}_2$  have been interpreted to show a transition to a highly incompressible phase above 100 GPa, this is not consistent with our static equation of state data.

DOI: [10.1103/PhysRevB.81.174121](https://doi.org/10.1103/PhysRevB.81.174121)

PACS number(s): 61.50.Ks, 62.50.–p, 64.30.Jk, 91.60.Gf

## I. INTRODUCTION

The  $\text{AX}_2$  family includes a variety of compounds of interest in geosciences, materials science, and condensed-matter physics that exhibit extensive polymorphism dependent on ionic size, electronic properties, and pressure.<sup>1</sup> One common highly coordinated polymorph is the fluorite structure, which is the stable polymorph at ambient conditions for the alkaline earth fluorides  $\text{CaF}_2$ ,  $\text{SrF}_2$ , and  $\text{BaF}_2$ . Fluorides are widely used as windows and lenses, optical coatings, scintillators, and luminescent materials.<sup>2</sup> At high pressures,  $\text{CaF}_2$  has been proposed as a pressure calibration standard.<sup>3,4</sup> The high coordination of the alkaline earth fluorides at ambient conditions can be analogous to the structure of lower coordination  $\text{AX}_2$  compounds at high pressure, including oxides relevant to geoscience and planetary science.<sup>1</sup> High-pressure studies on  $\text{CaF}_2$ ,  $\text{SrF}_2$ , and  $\text{BaF}_2$  have addressed band structure,<sup>5–11</sup> metallization,<sup>5–9,11,12</sup> optical properties,<sup>5,6,9,11</sup> melting behavior,<sup>13</sup> shear strength,<sup>14</sup> phase transitions,<sup>5,6,10,11,15–18</sup> and elastic properties.<sup>10,11,15,19–23</sup> The relative simplicity of the  $\text{AF}_2$  system makes it well suited for evaluating differences between theoretical and experimental studies of these properties.

The alkaline earth fluorides undergo a series of pressure-induced phase transitions to highly coordinated  $\text{AX}_2$  structures. At ambient conditions,  $\text{CaF}_2$ ,  $\text{SrF}_2$ , and  $\text{BaF}_2$  all crystallize in the cubic fluorite structure ( $Fm\bar{3}m$ ,  $Z=4$ ), which consists of a cubic close-packed array of cations with anions occupying tetrahedral sites. Experiments have shown that these materials transform to the orthorhombic cotunnite-type

structure ( $Pnam$ ,  $Z=4$ ) at 9 GPa, 5 GPa, and 3 GPa, respectively.<sup>24–27</sup> The cotunnite structure is characterized by anions in a distorted hexagonal-close-packed (hcp) lattice. The cations are situated within tricapped trigonal prisms with the three outer anions in the plane of the cation. An additional phase transition from the cotunnite phase to a hexagonal anti- $\text{Ni}_2\text{In}$ -type phase ( $P6_3/mmc$ ,  $Z=2$ ) has been found experimentally in  $\text{BaF}_2$  at 12 GPa by Leger *et al.*<sup>16</sup> The anti- $\text{Ni}_2\text{In}$ -type structure is a subgroup of the cotunnite structure with an ideal hcp anion lattice. The higher-symmetry lattice incorporates two more anions in the plane of the cations, forming pentacapped prisms. The transition sequence from fluorite to cotunnite-type to  $\text{Ni}_2\text{In}$ -type thus involves an increase in the coordination number from 8 to 9 to 11. These structures are also common in oxides at higher pressures. Cotunnite-type phases have been synthesized for  $\text{TiO}_2$ ,<sup>28,29</sup>  $\text{SnO}_2$ ,<sup>30</sup>  $\text{PbO}_2$ ,<sup>31</sup>  $\text{ZrO}_2$ ,<sup>32,33</sup>  $\text{HfO}_2$ ,<sup>32,34</sup> and  $\text{CeO}_2$ ,<sup>35</sup> and *ab initio* theory predicts  $\text{SiO}_2$  will transform to the cotunnite structure above 750 GPa.<sup>36</sup> Such high pressures are difficult to access experimentally, so information about the properties of high coordination phases of silica and other oxides must be derived either by theoretical methods or by experiments on analogs, such as fluorides.

As a model ionic system with useful physical properties, the alkaline earth fluorides have been extensively studied by *ab initio* and atomistic theoretical methods.<sup>5–13,17–19</sup> Theoretical studies have provided predictions of the phase transitions and equations of state for  $\text{CaF}_2$ ,<sup>5,7,10,11,19</sup>  $\text{SrF}_2$ ,<sup>6,7,17</sup> and  $\text{BaF}_2$ .<sup>8,9,12,18</sup> Although the transition to the cotunnite-type phase at high pressure is well known in  $\text{CaF}_2$  and  $\text{SrF}_2$ , the

compressibility of these materials is poorly constrained. For  $\text{CaF}_2$ , theoretical predictions of the zero-pressure bulk modulus of the cotunnite phase span a wide range from 66 to 154 GPa, and thus it is not clear whether the transition from fluorite ( $K_0=82$  GPa) to cotunnite involves a modest decrease or a large increase in the bulk modulus. Available experimental data<sup>15</sup> suggest a relatively high bulk modulus ( $K_0=170$  GPa) for the cotunnite-type phase of  $\text{CaF}_2$ . The situation is similar for  $\text{SrF}_2$ , where theoretical predictions of  $K_0$  for the cotunnite phase span a wide range, but in this case there is no experimental data for comparison.

At higher pressures, the transition to the  $\text{Ni}_2\text{In}$ -type phase previously found in  $\text{BaF}_2$  (Ref. 16) has been predicted in  $\text{CaF}_2$  and  $\text{SrF}_2$ . Theoretical studies<sup>5,10,11</sup> of  $\text{CaF}_2$  predict transition pressures to the  $\text{Ni}_2\text{In}$  phase that vary between 68 and 278 GPa. For  $\text{SrF}_2$ , the transformation has recently been predicted to occur at about 46 GPa.<sup>6</sup> No experimental studies yet exist to compare with these theoretical findings. Existing theoretical studies<sup>5,6,10,11</sup> predict values of the zero-pressure bulk modulus for 11-coordinated  $\text{Ni}_2\text{In}$ -type  $\text{SrF}_2$  and  $\text{CaF}_2$  that are comparable or even lower than values for the eight-coordinated fluorite phase. Experimental data<sup>12</sup> on  $\text{BaF}_2$  in a quasihydrostatic (He) pressure medium also yield a low bulk modulus for the  $\text{Ni}_2\text{In}$  phase in this composition, in contrast to earlier nonhydrostatic results.<sup>16</sup> Thus, these compounds appear to exhibit surprisingly high compressibilities for dense, highly coordinated high-pressure phases. These results stand in contrast to shock compression studies that suggest fluorides such as  $\text{CaF}_2$  transform to remarkably incompressible phases above 100 GPa.<sup>37,38</sup>

In other systems such as dioxides, diborides, and dinitrides, highly coordinated  $\text{AX}_2$  compounds have been synthesized at high pressure and are associated with low compressibilities. High-pressure phases of  $\text{TiO}_2$ ,<sup>28,29</sup>  $\text{ReB}_2$ ,<sup>39</sup> and  $\text{IrN}_2$ <sup>40</sup> have been examined as potential ultrahard or ultra-incompressible materials. The cotunnite phase of  $\text{TiO}_2$  has been reported to be both highly incompressible and hard with a zero-pressure bulk modulus of 294–431 GPa (Refs. 41–43) and a measured Vickers microhardness of 38 GPa.<sup>41</sup> The compressibility of corresponding fluoride phases is not yet well known.

In this work, we use x-ray diffraction in the laser-heated diamond-anvil cell (DAC) to investigate the equation of state and phase stability in  $\text{CaF}_2$ ,  $\text{SrF}_2$ , and  $\text{BaF}_2$  to Mbar pressures to provide new experimental constraints on the properties of high-pressure phases in this system. The results are used to explore the systematic high-pressure behavior of  $\text{AX}_2$  fluorides and compare with theoretical predictions.

## II. METHOD

Powder samples of  $\text{CaF}_2$  (99.985% purity) and  $\text{SrF}_2$  (99.99%) were obtained from Alfa Aesar and  $\text{BaF}_2$  (99.99%) from Sigma-Aldrich. X-ray diffraction confirmed that each material was in the fluorite-type structure and no impurities or other phases were detectable. Zero-pressure volumes were measured to be 163.6(2)  $\text{\AA}^3$ , 195.7(2)  $\text{\AA}^3$ , and 238.3(2)  $\text{\AA}^3$  for  $\text{CaF}_2$ ,  $\text{SrF}_2$ , and  $\text{BaF}_2$ , respectively.

High-pressure experiments were performed using synchrotron x-ray diffraction in a DAC. The samples were

ground to a few micron grain size and mixed with 10–15 wt % platinum (99.9% purity, 0.5–1.2  $\mu\text{m}$  particle size, Aldrich) as a laser absorber and pressure calibrant. A foil of the fluoride mixture was loaded into a symmetric DAC, sandwiched between two NaCl foils to provide a quasihydrostatic pressure medium and thermal insulation during laser heating.<sup>44</sup> For one  $\text{CaF}_2$  sample, we used a pressurized gas loading system<sup>45</sup> to load a Ne medium, with a NaCl foil supporting the sample on one side.

For experiments at pressures up to about 65 GPa, we used diamond anvils with 300  $\mu\text{m}$  culets, with the sample placed in a 150  $\mu\text{m}$  hole in a stainless steel gasket. In higher-pressure experimental runs, we used 200  $\mu\text{m}$  flat culet or 300/100  $\mu\text{m}$  or 300/75  $\mu\text{m}$  beveled culet diamond anvils. In these runs, we used rhenium gaskets with a 90  $\mu\text{m}$ , 50  $\mu\text{m}$ , or 25  $\mu\text{m}$  sample chamber, respectively. Gaskets were preindented to 25  $\mu\text{m}$  thickness before sample loading. Anvils were supported by either tungsten carbide seats with 50° conical holes or x-ray transparent cubic boron nitride seats with 33° conical holes.

Angle-dispersive x-ray diffraction with laser heating was performed at beamlines X17B3 of the National Synchrotron Light Source (NSLS) and 13-ID-D of the GSECARS sector and 16-ID-B of the HPCAT sector of the Advanced Photon Source (APS). At all facilities the x-ray beam was focused with a Kirkpatrick-Baez double mirror system. At X17B3, the x-ray beam size was approximately  $20 \times 30 \mu\text{m}$ , while at GSECARS, the beam size was  $5 \times 6 \mu\text{m}$  and at HPCAT,  $5 \times 10 \mu\text{m}$ . The detector at X17B3 was either an offline Fuji BAS2500 image plate or an online Mar345 image plate. At GSECARS and HPCAT we used a MarCCD charge-coupled device detector. The distance and orientation of the detector was calibrated using a  $\text{CeO}_2$  standard; at X17B3, an Au standard was also used for confirmation and simultaneous wavelength calibration.

Table I lists all experimental runs reported in this study. We conducted both compression and decompression experiments. Laser annealing was required for equation of state measurements since the NaCl medium is not sufficient by itself to provide quasihydrostatic conditions. All samples were heated from both sides at high pressures with a Nd:YLF (neodymium:yttrium lithium fluoride) or Nd:YAG (neodymium:yttrium aluminum garnet) laser.<sup>46,47</sup> Temperatures were measured by spectroradiometry.<sup>48</sup> Heating was carried out to temperatures ranging from 1500 to 3000 K for typical durations of 20 min. For one  $\text{CaF}_2$  run, we heated the sample with a Nd:YLF laser at the MIT Mineral Physics Laboratory, and then decompressed without additional heating at X17B3. After heating, Debye rings from fluoride samples were smooth, indicating little preferred orientation. Diffraction peak widths sharpened significantly due to heating: an unheated sample at 82 GPa showed a reduction in peak full width at half maximum of over 50% after heating.

Two-dimensional diffraction images were radially integrated using FIT2D software<sup>49</sup> to produce one-dimensional diffraction patterns. To obtain peak positions, widths, and intensities, patterns were fit with background-subtracted Voigt line shapes. Lattice parameters were refined for all data using UNITCELL.<sup>50</sup> Rietveld refinement of selected patterns was conducted using GSAS and EXPGUI software.<sup>51,52</sup>

TABLE I. Summary of experimental runs.

Material	Beamline	Detector	Culet, gasket hole ( $\mu\text{m}$ )	Pressure range (GPa)	$P$ - $T$ path
CaF <sub>2</sub>	APS GSECARS 13-ID-D	CCD	200, 90	13–95	Compression with laser heating above 82 GPa
CaF <sub>2</sub>	APS GSECARS 13-ID-D	CCD	300, 150	4–64	Compression with laser heating above 45 GPa
CaF <sub>2</sub>	NSLS X17B3	Image plate	200, 90	56–84	Heating, cold decompression
CaF <sub>2</sub>	APS GSECARS 13-ID-D	CCD	300/75, 25	90–146	Heated compression
CaF <sub>2</sub>	APS GSECARS 13-ID-D	CCD	300, 150	15–60	Heated compression in Ne medium
SrF <sub>2</sub>	NSLS X17B3	Image plate	200, 90	58–89	Heated compression
SrF <sub>2</sub>	APS GSECARS 13-ID-D	CCD	300, 150	9–64	Heated compression, heated decompression
BaF <sub>2</sub>	APS HPCAT 16-ID-B	CCD	300/100, 50	4–133	Heated compression

Pressure was determined from the equation of state of platinum.<sup>53</sup> Measured lattice strains in Pt were also used to evaluate differential stress,  $t$ , following the theory by Singh.<sup>54</sup> In the presence of differential stress, the elastic anisotropy  $S$  of Pt results in systematic variations in diffraction lines as a function of lattice plane,  $hkl$ . For a pair of reflections at similar diffraction angle,  $2\theta$ , Singh's equations for lattice strain in a cubic crystal in an axial, angle-dispersive geometry can be approximated<sup>55</sup> as

$$\frac{a_{hkl} - a_{hkl}^*}{a_0} \approx -S[1 - 3 \cos^2(90^\circ - \theta_{hkl})][\Gamma(hkl) - \Gamma(hkl^*)],$$

where  $a$  is the lattice parameter for a given  $hkl$ ,  $a_0$  is the lattice parameter at ambient pressure, and  $\Gamma$  is  $(h^2k^2 + k^2l^2 + l^2h^2)/(h^2 + k^2 + l^2)^2$ . The angular proximity and strong intensity of the Pt 111 and 200 peaks make them ideal for this analysis. The elastic anisotropy of Pt as a function of pressure was taken from *ab initio* calculations<sup>56</sup> which we fit to an exponential relation:  $S(P) = 0.0012 + 0.0027 \exp(-0.0058P)$ , where  $P$  is in gigapascal and  $S$  in inverse gigapascal. This analysis showed that laser annealing reduced differential stress to less than 1 GPa in Pt. Only annealed data were used in equation of state fits.

### III. RESULTS

#### A. Phase identification

Representative high-pressure diffraction patterns for CaF<sub>2</sub>, SrF<sub>2</sub>, and BaF<sub>2</sub> are shown in Figs. 1–3. All patterns can be indexed to the cubic fluorite phase, the orthorhombic cotunnite-type phase,<sup>20,24,25</sup> or the hexagonal Ni<sub>2</sub>In-type phase.<sup>16</sup> Representative comparisons of measured and fit  $d$  spacings for the cotunnite and Ni<sub>2</sub>In phases of CaF<sub>2</sub> are shown in Tables II and III. No other phases were observed up to 146 GPa in CaF<sub>2</sub>, 89 GPa in SrF<sub>2</sub>, and 133 GPa in BaF<sub>2</sub>, either at 300 K or during laser heating at 1500–2500 K. For BaF<sub>2</sub>, a sample heated to 3000 K at 111 GPa showed additional weak peaks that were preserved up to 133 GPa with further heating and may be due to a reaction between the sample and the surrounding materials.

For all samples, the fluorite-cotunnite phase transition was observed to occur without heating. The observed transition pressure for our room-temperature compression of CaF<sub>2</sub> and

SrF<sub>2</sub> is higher than that in other studies;<sup>12,15,16,24–27</sup> this reflects variations in metastable behavior under different degrees of differential stress. During initial pressurization of the DAC, BaF<sub>2</sub> was compressed to 3.8 GPa, and the transition from fluorite to cotunnite-type was already completed at this pressure.

Our study has experimentally identified the Ni<sub>2</sub>In-type phase in SrF<sub>2</sub> and CaF<sub>2</sub>. In SrF<sub>2</sub>, the orthorhombic cotunnite-type phase transformed to the hexagonal Ni<sub>2</sub>In-type phase upon compression at 36 GPa with heating to about 1500 K. The new phase was maintained upon decompression with heating down to 29 GPa. At 28 GPa, diffraction patterns measured during heating to 1500–2000 K exhibited the Ni<sub>2</sub>In-type phase, but upon quench the SrF<sub>2</sub> sample had returned to the cotunnite structure. This is evidence that the cotunnite to Ni<sub>2</sub>In-type transition has a negative Clapeyron slope but uncertainty in temperature measurement makes the slope difficult to quantify. Another SrF<sub>2</sub> sample compressed directly to 58 GPa without heating displayed broad diffraction peaks consistent with the Ni<sub>2</sub>In-type phase that sharpened with subsequent heating. CaF<sub>2</sub> transformed from the cotunnite-type phase to the Ni<sub>2</sub>In-type phase at 79 GPa with

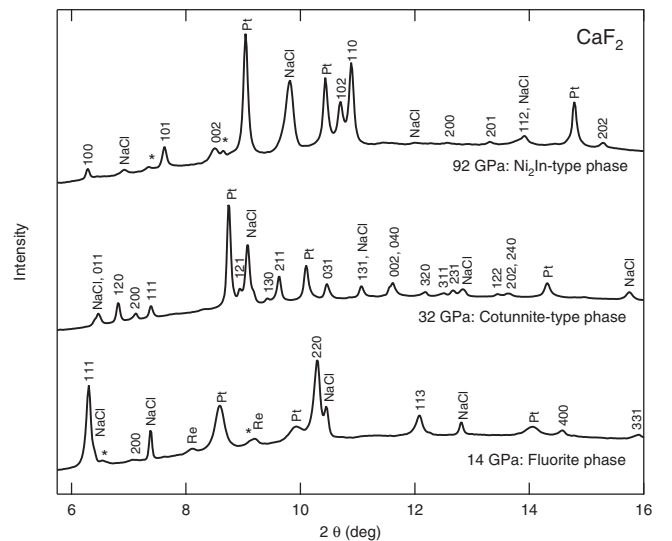


FIG. 1. Representative x-ray diffraction patterns for CaF<sub>2</sub>. Peaks labeled with asterisks in fluorite and Ni<sub>2</sub>In-type patterns are from minor amounts of the cotunnite-type phase.

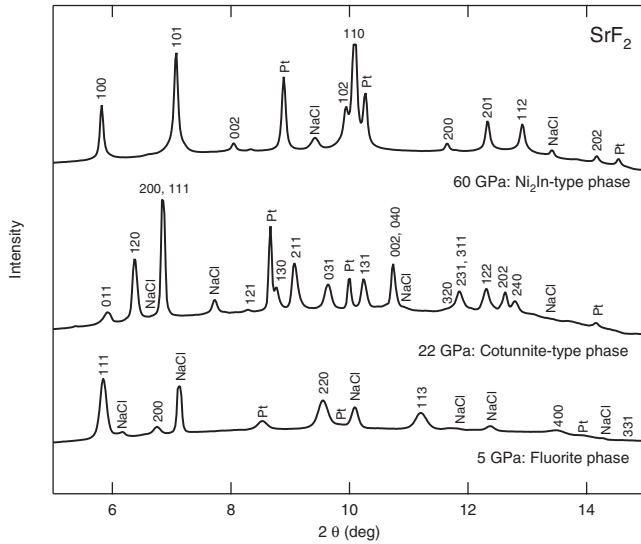


FIG. 2. Representative x-ray diffraction patterns for  $\text{SrF}_2$ .

heating to about 2000 K. Upon decompression without heating, diffraction peaks remained sharp to 72 GPa but broadened significantly at lower pressures and the sample appeared to become partially amorphous. Laser heating at 63 GPa produced the cotunnite phase. For all compositions, the  $\text{Ni}_2\text{In}$ -type phase could not be recovered to ambient pressure. Based on our temperature-quenched diffraction patterns, these experiments constrain the cotunnite- $\text{Ni}_2\text{In}$ -type transition pressure at 300 K to 28–29 GPa for  $\text{SrF}_2$  and 63–79 GPa for  $\text{CaF}_2$ .

The transition from the cotunnite-type to  $\text{Ni}_2\text{In}$ -type phase in  $\text{CaF}_2$  and  $\text{SrF}_2$  has also been investigated at 0 K by theoretical studies using density-functional theory.<sup>5,6,10,11</sup> For  $\text{CaF}_2$ , our results are more consistent with the predicted transition pressure found by Wu *et al.*<sup>5</sup> (68–72 GPa) than by Shi *et al.*<sup>10</sup> (105 GPa) or Cui *et al.*<sup>11</sup> (278 GPa). For  $\text{SrF}_2$ , the transition occurred at pressures lower than predicted (45.6 GPa).<sup>6</sup> Some of the differences in phase-transition pressures

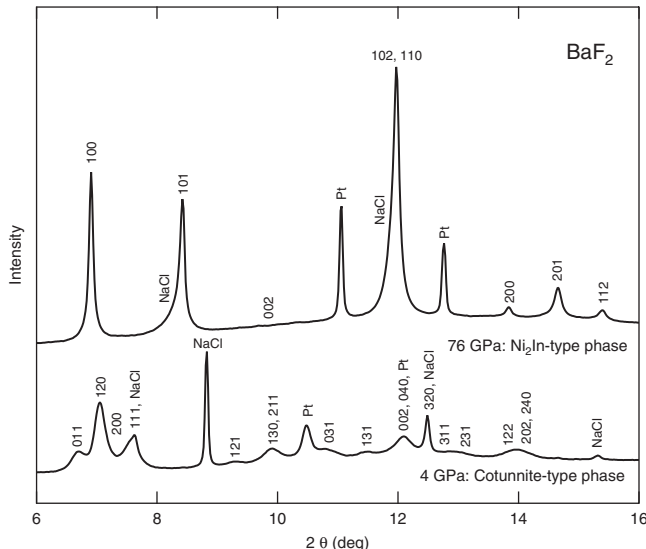


FIG. 3. Representative x-ray diffraction patterns for  $\text{BaF}_2$ .

between experiment and theory may reflect thermal effects. While the negative Clapeyron slope observed does support higher transition pressures at 0 K than at 300 K, this is unlikely to account for more than a few gigapascal difference. More critical to the accuracy of these predicted transition pressures is the similarity between the cotunnite and  $\text{Ni}_2\text{In}$ -type phases and their calculated enthalpies. A small enthalpy difference between these structures over a wide pressure range as observed in these calculations makes the transition pressure particularly sensitive to error in computational parameters. Such a small enthalpy difference would also increase the dependence of experimental results on temperature, differential stress, and kinetics.

The  $\text{Ni}_2\text{In}$ -type structure of  $\text{SrF}_2$  at 58.4 GPa was confirmed by full profile refinement (Fig. 4). Except for a broad unknown peak with a  $2\theta$  value of approximately  $8^\circ$ , all peaks could be indexed as NaCl B2 phase, Pt, or  $\text{SrF}_2$  in the  $\text{Ni}_2\text{In}$  structure. Lattice parameters, phase fractions, peak shape parameters, and spherical harmonic terms were refined for all phases. As all atoms are in special positions, no refinement of atomic positions was necessary. The texture index was 1 for NaCl, 1.11 for Pt, and 3.47 for  $\text{SrF}_2$  indicating substantial preferred orientation, with the (001) plane aligned normal to the compression direction. The refinement yielded lattice parameters  $a=3.8130(2)$  Å and  $c=4.7788(21)$  Å, and a volume of  $60.171(26)$  Å<sup>3</sup>, consistent with values obtained by individual peak fitting to within 0.1%.

## B. Equation of state

Unit-cell volumes for  $\text{CaF}_2$ ,  $\text{SrF}_2$ , and  $\text{BaF}_2$  were fit to a third-order Birch-Murnaghan equation of state and the results are shown in Fig. 5 and Tables IV and V. It is well known that volume compression data may suffer from trade-offs in constraining the three zero-pressure parameters of the equation of state, volume  $V_0$ , bulk modulus  $K_0$ , and pressure derivative of the bulk modulus  $K'_0$ . In order to better constrain  $K_0$ , we fixed  $V_0$  or  $K'_0$ . Most of the uncertainty in the fit comes from poor constraint on  $V_0$ . Fixing the zero-pressure volume of the high-pressure phases to various values based on previous experimental or theoretical results (Tables IV and V) results in a range of values for  $K_0$  and  $K'_0$ . This range illustrates the error in our constraint of these zero-pressure equation of state parameters due to parameter trade-offs. Alternatively,  $K'_0$  may be fixed to a reasonable value based on previous work. Previous experimental and theoretical work on  $\text{CaF}_2$ ,  $\text{SrF}_2$ , and  $\text{BaF}_2$  found that  $K'_0$  is 4.67–4.7 for all phases of  $\text{BaF}_2$ ,<sup>12</sup> 4.75 for the fluorite phase of  $\text{SrF}_2$ ,<sup>21</sup> and 4.38–4.83 for all phases of  $\text{CaF}_2$ ,<sup>11,22</sup> suggesting that  $K'_0$  may have little variation with structure or cation for the alkaline earth fluorides. We therefore chose a  $K'_0$  of 4.7 when using a fixed value for this parameter in our fits.

### 1. Cotunnite-type phase

The results of equation of state fits for the cotunnite phases of  $\text{CaF}_2$  and  $\text{SrF}_2$  are compared with earlier studies in Table IV. With  $K'_0$  fixed at 4.7, the zero-pressure volumes of the cotunnite-type phases of  $\text{CaF}_2$  and  $\text{SrF}_2$  are 6–10 % less than  $V_0$  of the corresponding fluorite phases at ambient con-

TABLE II. Observed and calculated  $d$  spacings for the cotunnite-type phase of  $\text{CaF}_2$  at 35 GPa and 300 K. These peaks are fit to an orthorhombic unit cell with  $a=5.3869(10)$  Å,  $b=6.5955(13)$  Å,  $c=3.3149(7)$  Å, and  $V=117.78(3)$  Å<sup>3</sup>.

$h$	$k$	$l$	$d_{\text{obs}}$ (Å)	$d_{\text{calc}}$ (Å)	$\Delta d$ (Å)	Intensity (%)
0	1	1	2.96239	2.96183	0.00056	47
1	2	0	2.81191	2.81259	-0.00068	82
2	0	0	2.69359	2.69347	0.00012	26
1	1	1	2.59449	2.5954	-0.00091	48
1	2	1	2.14467	2.14463	0.00004	50
2	0	1	2.09014	2.0904	-0.00026	31
1	3	0	2.03592	2.03552	0.0004	12
2	1	1	1.99243	1.99271	-0.00028	100
0	3	1	1.83303	1.83218	0.00085	63
1	3	1	1.73396	1.73459	-0.00063	48
3	2	0	1.57698	1.57702	-0.00004	16
3	1	1	1.53659	1.5355	0.00109	10
2	3	1	1.51534	1.51491	0.00043	23
1	2	2	1.42777	1.42794	-0.00017	9

ditions. For  $\text{CaF}_2$ , this is consistent with density-functional theory<sup>5,10,11</sup> and with the measured volume of cotunnite-type  $\text{CaF}_2$  synthesized at ambient conditions<sup>57</sup> or recovered from shock compression.<sup>58</sup> It is also consistent with the volume difference between cotunnite and fluorite obtained in recent work on  $\text{BaF}_2$ .<sup>12</sup>

With a zero-pressure bulk modulus of 74(5) GPa, the cotunnite phase of  $\text{CaF}_2$  is slightly more compressible than the fluorite phase. The same relationship was recently found between the cotunnite and fluorite phases of  $\text{BaF}_2$  by Smith *et al.*<sup>12</sup> A previous static compression experiment<sup>15</sup> on  $\text{CaF}_2$  yielded a much higher bulk modulus for the cotunnite phase ( $K_0=170$  GPa). The presence of differential stress is known to lead to overestimation of the bulk modulus in static compression studies;<sup>59</sup> this is the most likely explanation for the discrepancy as the results of Ref. 15 were obtained from an unannealed sample in a methanol-ethanol medium at up to 45 GPa, well above the pressure limit of the hydrostaticity of this medium.<sup>60</sup> Similar results are found in the case of  $\text{BaF}_2$ , where a more recent experiment<sup>12</sup> conducted with a quasihy-

drostatic He pressure medium yielded a much lower bulk modulus for the cotunnite-type phase than earlier work of Leger *et al.*<sup>16</sup> with a silicone grease medium. For the cotunnite phase of  $\text{SrF}_2$ , fewer data and the narrower pressure stability range give a poorer constraint on  $K_0$ , but the fit is consistent with the trend seen in  $\text{CaF}_2$  and  $\text{BaF}_2$ . The bulk modulus of 74(8) GPa is within uncertainty from the bulk modulus of the fluorite phase of  $\text{SrF}_2$ . The fit value of  $V_0$  for the cotunnite phase yields a volume relative to the fluorite phase of  $V_0(\text{cotunnite})/V_0(\text{fluorite})=0.90(1)$ , which is lower than the values for either  $\text{CaF}_2$  or  $\text{BaF}_2$ . If  $V_0$  is fixed to a value of 150.5 Å<sup>3</sup> [ $V_0(\text{cotunnite})/V_0(\text{fluorite})=0.92$  between the relative volumes for  $\text{CaF}_2$  and  $\text{BaF}_2$ ], then the fit value of  $K_0$  becomes 62(1) GPa, between the  $K_0$  values for  $\text{CaF}_2$  and  $\text{BaF}_2$ .<sup>12</sup>

The similar compressibility of fluorite and cotunnite forms of  $\text{CaF}_2$  is consistent with recent density-functional theory calculations,<sup>5,10,11</sup> for which generalized gradient approximation (GGA) calculation gives better quantitative agreement with  $K_0$  than the local-density approximation.

TABLE III. Observed and calculated  $d$  spacings for the  $\text{Ni}_2\text{In}$ -type phase of  $\text{CaF}_2$  at 92 GPa and 300 K. These peaks are fit to a hexagonal unit cell with  $a=3.5230(5)$  Å,  $c=4.4337(10)$  Å, and  $V=47.66(2)$  Å<sup>3</sup>.

$h$	$k$	$l$	$d_{\text{obs}}$ (Å)	$d_{\text{calc}}$ (Å)	$\Delta d$ (Å)	Intensity (%)
1	0	0	3.05045	3.05104	-0.00059	9
1	0	1	2.51439	2.51342	0.00097	27
0	0	2	2.21665	2.21683	-0.00018	7
1	0	2	1.79308	1.79342	-0.00034	66
1	1	0	1.76184	1.76152	0.00032	100
2	0	1	1.44230	1.44252	-0.00022	6
2	0	2	1.25698	1.25671	0.00027	7

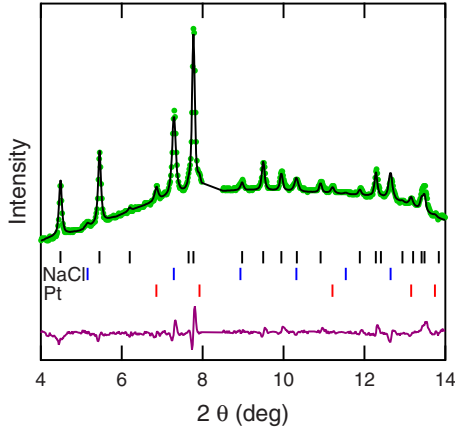


FIG. 4. (Color online) Full profile refinement of  $\text{SrF}_2$   $\text{Ni}_2\text{In}$ -type phase with  $P6_3/mmc$  symmetry and atomic positions Sr:  $(1/3, 2/3, 1/4)$ , F:  $(0, 0, 0)$ , and  $(1/3, 2/3, 3/4)$ . Refined fit curve is superimposed on measured intensities (dots), with the residual curve below. Vertical ticks mark peak positions for  $\text{SrF}_2$   $\text{Ni}_2\text{In}$ -type, NaCl B2, and Pt phases.

Other theoretical calculations for  $\text{CaF}_2$  and  $\text{SrF}_2$  suggest a much higher<sup>6,7</sup> bulk modulus for the cotunnite phase. The same has been found for  $\text{BaF}_2$ : the most recent calculations for  $\text{BaF}_2$  using the GGA method yield a bulk modulus for the cotunnite-type phase in good agreement with experimental data obtained under hydrostatic conditions,<sup>12</sup> but earlier theoretical results using other techniques<sup>8,9,18</sup> predicted a higher bulk modulus. Experiments conducted under hydrostatic conditions and recent theoretical work thus appear to be converging on compressibility for the cotunnite-type phase comparable to that of the fluorite phase.

Figure 6 shows variation in lattice parameters with pressure for the cotunnite phases of  $\text{CaF}_2$ ,  $\text{SrF}_2$ , and  $\text{BaF}_2$ . Near the upper pressure limit of the stability of the cotunnite-type phase, in well-annealed samples we observed a continuous change in the lattice parameters of the orthorhombic unit cell

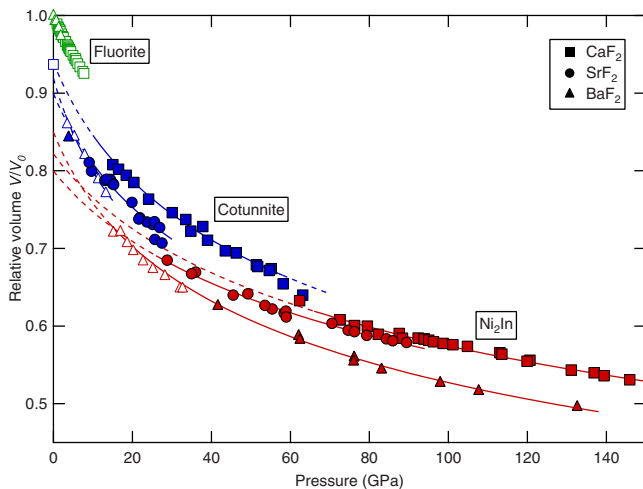


FIG. 5. (Color online) Compression curves and Birch-Murnaghan equation of state fits for  $\text{CaF}_2$ ,  $\text{SrF}_2$ , and  $\text{BaF}_2$ . Open symbols are from previous experimental work (Refs. 4, 12, and 57). All data are plotted relative to  $V_0$  of the fluorite phase.

with a discontinuous change in the axial compressibilities. Above 55 GPa, the  $c$  lattice parameter expands with increasing pressure, but a more rapid increase in compressibility of the  $a$  parameter results in a net increase in volumetric compressibility (Fig. 5). Figure 7 shows a direct comparison of interplanar spacings across the cotunnite- $\text{Ni}_2\text{In}$  phase transition for the three alkaline earth fluorides. This phenomenon was also observed by Smith *et al.*<sup>12</sup> in  $\text{BaF}_2$  and predicted by Ayala<sup>18</sup> in  $\text{BaF}_2$  and Kunc *et al.*<sup>61</sup> in  $\text{Li}_2\text{O}$  (anticotunnite). Consistent with the group-subgroup relationship between the cotunnite and  $\text{Ni}_2\text{In}$ -type structures, we observe a continuous evolution of the orthorhombic structure toward the hexagonal structure near the phase transition. However, the hysteresis without laser heating and the 5% volume change with heating observed across the transition to the hexagonal phase for all three alkaline earth fluorides indicate that this phase transition is first order.

## 2. $\text{Ni}_2\text{In}$ -type phase

Table V summarizes equation of state parameters for the  $\text{Ni}_2\text{In}$  phase of  $\text{CaF}_2$ ,  $\text{SrF}_2$ , and  $\text{BaF}_2$ . The  $\text{Ni}_2\text{In}$  phase of  $\text{BaF}_2$  is constrained over the widest range of experimental data from its transition pressure at 12 GPa (Ref. 16) to our maximum pressure of 133 GPa. The equation of state described by our annealed data (shown in Fig. 5) from 42–133 GPa matches well with the measurement in a He pressure medium by Smith *et al.* from 15–33 GPa:  $K_0$  is 67(9) GPa and  $V_0$  is 202(4)  $\text{\AA}^3$ , 85% of the fluorite  $V_0$ . This bulk modulus is comparable to Smith *et al.*'s theoretical and experimental values<sup>12</sup> but significantly lower than values measured by Leger *et al.*<sup>16</sup> and earlier theoretical calculations.<sup>8,9,18</sup> The  $\text{Ni}_2\text{In}$ -type phase of  $\text{BaF}_2$  has the same zero-pressure bulk modulus as the cotunnite-type phase within experimental error.

Because the  $\text{Ni}_2\text{In}$ -type phases of  $\text{CaF}_2$  and  $\text{SrF}_2$  are stable only at higher pressures and become amorphous or transform to the cotunnite-type phase upon decompression, the zero-pressure equation of state parameters for these phases are more difficult to constrain. A wide range of values for  $V_0$ ,  $K_0$ , and  $K'_0$  reproduce the high-pressure data. Fitting results with either  $V_0$  or  $K'_0$  fixed are shown in Table V. Constraints on  $V_0$  and  $K'_0$  are based on theoretical work and analogous experiments on  $\text{BaF}_2$ . The choice of these constraints strongly controls  $K_0$ . It is difficult to compare fit values for  $V_0$  or  $K_0$  to theoretical work<sup>5,10,11</sup> as most studies do not report  $K'_0$ . Our fit for  $\text{CaF}_2$  agrees with theoretical values for  $V_0$  and  $K_0$  only if  $K'_0$  is high, about 5.9. Our results for  $\text{SrF}_2$  are not consistent with theoretical work.<sup>6</sup> Either  $K_0$  or  $K'_0$  must be higher for the  $\text{Ni}_2\text{In}$ -type phase than the cotunnite phase to fit the  $\text{CaF}_2$  and  $\text{SrF}_2$  data, unlike  $\text{BaF}_2$ , for which neither  $K_0$  nor  $K'_0$  were significantly different for the fluorite, cotunnite, and  $\text{Ni}_2\text{In}$ -type phases. Theoretical studies<sup>5,6,10,11</sup> did not predict an increase in bulk modulus for the  $\text{Ni}_2\text{In}$ -type phase; instead, the bulk modulus was predicted to be less than or similar to that of the cotunnite phase, as in  $\text{BaF}_2$ . The compositional trend in the zero-pressure bulk modulus roughly shows higher  $K_0$  for smaller cations but cannot be unambiguously resolved due to the parameter trade-offs.

TABLE IV. Birch-Murnaghan equation of state parameters for fluorite and cotunnite phases of alkaline earth fluorides from this and previous studies. Moduli from Brillouin scattering and ultrasonic studies have been corrected from adiabatic to isothermal values.  $V_0$  for fluorite-type  $\text{CaF}_2$ ,  $\text{SrF}_2$ , and  $\text{BaF}_2$  are  $163.6 \pm 0.2 \text{ \AA}^3$ ,  $195.7 \pm 0.17 \text{ \AA}^3$ , and  $238.3 \pm 0.2 \text{ \AA}^3$ , respectively.

Reference	$K_0$ (fluorite)		$K_0$ (cotunnite)		$V_0$ (cotunnite)/ $V_0$ (fluorite)
	(GPa)	$K'_0$ (fluorite)	(GPa)	$K'_0$ (cotunnite)	
			$\text{CaF}_2$		
This work			$74 \pm 5$	$4.7^a$	$0.94 \pm 0.01$
X-ray diffraction:					
Ref. 4	$81 \pm 1.2$	$5.22 \pm 0.35$			
Ref. 15	$87 \pm 5$	$5 \pm 1$	$169 \pm 8^b$	$4.7^{a,b}$	0.86
Ref. 57					0.937
Brillouin scattering <sup>22</sup>	$82.0 \pm 0.7$	$4.83 \pm 0.13$			
Theory <sup>5,7,10,11,19</sup>	77–103	4–4.92	66–153.8	4.1–4.38	0.863–0.937
			$\text{SrF}_2$		
This work			$74 \pm 8$	$4.7^a$	$0.90 \pm 0.01$
			$62 \pm 1$	$4.7^a$	$0.92^a$
Ultrasonics <sup>20,21</sup>	70–71	$4.76 \pm 0.06$			
Theory <sup>6,7</sup>	66–90		117–127		0.793–0.868
			$\text{BaF}_2$		
X-ray diffraction:					
Ref. 12			$51 \pm 4$	$4.7^a$	$0.92 \pm 0.01$
Ref. 16			$79 \pm 10$	$4^a$	$0.907 \pm 0.005$
Ultrasonics <sup>23</sup>	56.9				
Theory <sup>8,9,12,18</sup>	50–80	4.67–4.91	52–98	$4.7^c$	0.876–0.937

<sup>a</sup>Parameter fixed in fit.

<sup>b</sup>Birch-Murnaghan equation fit to reported diffraction data.

<sup>c</sup>Only Ref. 12 provides a value for  $K'_0$ .

To more directly compare the compressibilities of  $\text{CaF}_2$ ,  $\text{SrF}_2$ , and  $\text{BaF}_2$  in the same pressure regime as our data, we examine the bulk modulus,  $K$ , calculated at high pressures. Differentiation of the Birch-Murnaghan equation yields a third-order finite strain expression of the variation in  $K$  with compression.<sup>62</sup> Results for the three compositions under consideration here are calculated with the parameters given in Table V with  $K'_0$  fixed at 4.7 and shown in Fig. 8. The change in bulk modulus is small across the fluorite-cotunnite transition for all compositions and suggests the cotunnite phase can be more compressible than the fluorite phase. In contrast, for the cotunnite- $\text{Ni}_2\text{In}$  transition, there is a large increase in bulk modulus at the phase transition pressure. At the cotunnite- $\text{Ni}_2\text{In}$ -type phase transition pressure of 14 GPa, the bulk modulus,  $K$ (14 GPa), is 10–30% larger for the  $\text{Ni}_2\text{In}$ -type phase than for the cotunnite phase. This is greater than the bulk modulus contrast calculated from the experimental equation of state of Ref. 12 (7%), although both this previous work and our equations of state have volume  $V$ (14 GPa) for the  $\text{Ni}_2\text{In}$ -type phase 5% lower relative to the cotunnite-type phase.<sup>12</sup>  $\text{CaF}_2$  and  $\text{SrF}_2$  also display a 5% volume reduction across the cotunnite- $\text{Ni}_2\text{In}$ -type transition, although theoretical studies<sup>5,6,10,11</sup> predicted the volume

change would be 0–2.5% for these materials. For  $\text{CaF}_2$  and  $\text{SrF}_2$ , the change in the bulk modulus across the transition is greater than for  $\text{BaF}_2$ : the cotunnite- $\text{Ni}_2\text{In}$ -type transition results in a 20–40% ( $\text{CaF}_2$ ) to 45–65% ( $\text{SrF}_2$ ) increase in the bulk modulus. At 100 GPa, the  $\text{Ni}_2\text{In}$ -type phase has a bulk modulus of 240 GPa for  $\text{BaF}_2$ , 330 GPa for  $\text{SrF}_2$ , and 320 GPa for  $\text{CaF}_2$ . The higher bulk modulus values for  $\text{SrF}_2$  relative to  $\text{CaF}_2$  may reflect experimental uncertainty and require further investigation.

In previous experimental and theoretical studies on the  $\text{Ni}_2\text{In}$ -type phase of  $\text{BaF}_2$ ,<sup>12,16,18</sup> an anomalously high value of the bulk modulus has been shown to be linked with a systematically high value of the  $c$  lattice parameter and hence  $c/a$  ratio. Leger *et al.*<sup>16</sup> observed an increase in the  $c/a$  ratio with pressure, but their pressure transmitting medium, silicone grease, is nonhydrostatic above 0.9 GPa.<sup>60</sup> Theoretical work<sup>18</sup> predicted a decrease in  $c/a$  ratio with pressure and suggested that differential stress resulted in the  $c$  lattice parameter being less compressible than under hydrostatic conditions. Recent x-ray diffraction experiments by Smith *et al.*<sup>12</sup> comparing quasihydrostatic compression in a He medium to nonhydrostatic compression with no pressure medium confirm this. Measured volumes in a nonhydrostatic

TABLE V. Birch-Murnaghan equation of state parameters for Ni<sub>2</sub>In-type phases of alkaline earth fluorides from this and previous studies.

Reference	$K_0$ (GPa)	$K'_0$	$V_0(\text{Ni}_2\text{In-type})/V_0(\text{fluorite})$
CaF <sub>2</sub>			
This work	118 ± 11	4.7 <sup>a</sup>	0.82 ± 0.01
	95 ± 5	5.1 ± 0.3	0.85 <sup>a</sup>
	60 ± 5	5.9 ± 0.5	0.90 <sup>a</sup>
Theory (Refs. 5, 10, and 11)	61–91	4.8 <sup>b</sup>	0.890–0.925
SrF <sub>2</sub>			
This work	125 ± 9	4.7 <sup>a</sup>	0.80 ± 0.01
	64 ± 5	7.0 ± 0.6	0.85 <sup>a</sup>
	32 ± 4	10 ± 1.4	0.90 <sup>a</sup>
Theory (Ref. 6)	43.8		0.633
BaF <sub>2</sub>			
This work	67 ± 9	4.7 <sup>a</sup>	0.85 ± 0.02
X-ray diffraction			
Ref. 12	56 ± 5	4.67 <sup>a</sup>	0.86 ± 0.02
Ref. 16	133 ± 16	4 <sup>a</sup>	0.829 ± 0.012
Theory (Refs. 8, 9, 12, and 18)	69–142	4.67 <sup>c</sup>	0.753–0.864

<sup>a</sup>Parameter fixed in fit.

<sup>b</sup>Only Ref. 11 provides a value for  $K'_0$ .

<sup>c</sup>Only Ref. 12 provides a value for  $K'_0$ .

sample were as much as 10% greater than in a quasihydrostatic sample, creating the appearance of a much less com-

pressible phase. The volume difference between the two experiments is due almost entirely to the behavior of the  $c$  parameter.

In our experiments on all three compounds we find the  $c/a$  ratio of the Ni<sub>2</sub>In-type phase decreased with pressure as long as the sample was well annealed (Fig. 9). The  $c/a$  ratio increased significantly if differential stress was allowed to accumulate. We heated our BaF<sub>2</sub> sample at approximately 10–15 GPa intervals. The  $c$  parameter appears less compressible in these intervals than immediately after heating, as can be observed from the open symbols in Fig. 9. The  $c/a$  ratio of the Ni<sub>2</sub>In-type phase correlates well with diffraction peak widths and the normalized differential stress ( $t/P$ ) measured in platinum (Fig. 10): the linear correlation coefficient  $\rho = 0.69$ . This correlation is strong enough to suggest that the  $c/a$  ratio of BaF<sub>2</sub> could be used to calibrate differential stress above 12 GPa. While the differential stress in Pt could not be measured in SrF<sub>2</sub> experiments above 60 GPa due to overlap between Pt and sample diffraction peaks, peaks were slightly wider in this experimental run than other well-annealed runs, which may indicate less hydrostatic conditions, resulting in a higher  $c/a$  ratio and volume. However, the decrease in  $c/a$  ratio with pressure measured in both CaF<sub>2</sub> and SrF<sub>2</sub> may be evidence that the bulk modulus has not been overestimated here due to differential stress.

Experimental data provide an important test for theoretical studies. Theoretical calculations for the alkaline earth fluorides have used a variety of techniques from atomistic to *ab initio* simulations involving different levels of sophistica-

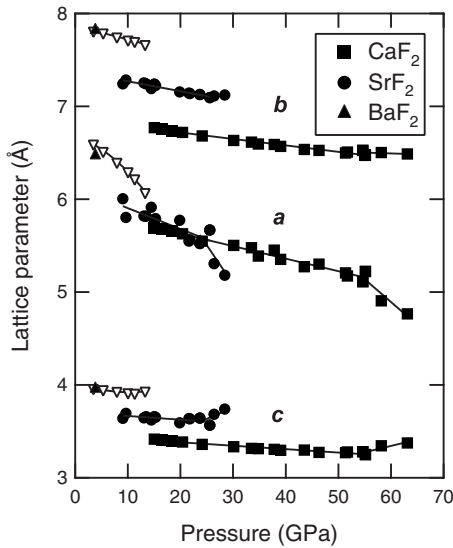


FIG. 6. Lattice parameters of the cotunnite-type phase of alkaline earth fluorides. Open triangles are from previous work in He medium (Ref. 12). Linear fits are shown as a guide to the eye. Near the upper stability limit, the structure distorts continuously toward the hexagonal phase: the  $a$  parameter becomes more compressible while  $c$  increases in magnitude.



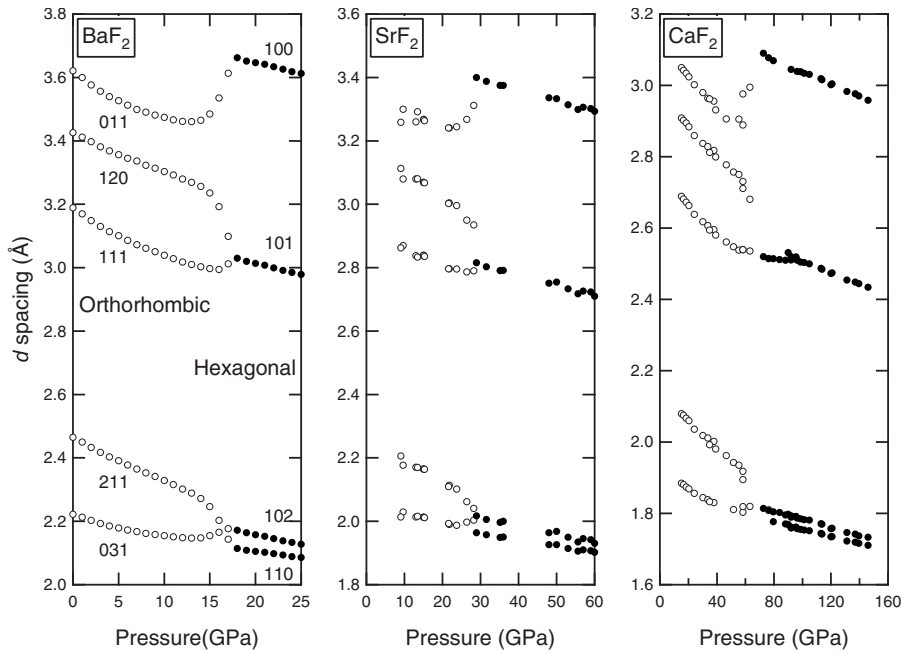


FIG. 7. Interplanar spacing variation across the cotunnite- $\text{Ni}_2\text{In}$  transition. Open symbols represent cotunnite-type phase diffraction peaks. Closed symbols are  $\text{Ni}_2\text{In}$ -type phase peaks.  $\text{CaF}_2$  and  $\text{SrF}_2$  data are from this study.  $\text{BaF}_2$  data are from molecular-dynamics simulation (Ref. 26).

tion. Among density-functional theory calculations, we find that results for  $\text{CaF}_2$  by Wu *et al.*<sup>5</sup> using GGA most closely matched our transition pressures. However, studies using the GGA method have produced a wide range of pressures for the cotunnite- $\text{Ni}_2\text{In}$ -type transition in  $\text{CaF}_2$ ,<sup>5,10,11</sup> and all predict bulk moduli lower than those we observe for the  $\text{Ni}_2\text{In}$ -type phases of  $\text{CaF}_2$  and  $\text{SrF}_2$ .<sup>5,6,10,11</sup> Theoretical studies on  $\text{BaF}_2$  had previously reported zero-pressure bulk moduli for the  $\text{Ni}_2\text{In}$ -type phase of over 133 GPa,<sup>8,9,18</sup> until Smith *et al.*<sup>12</sup> reported an experimental value of 56 GPa and confirmed a higher compressibility with their own GGA calculations. This highlights the importance of experimental confirmation of theoretical predictions.

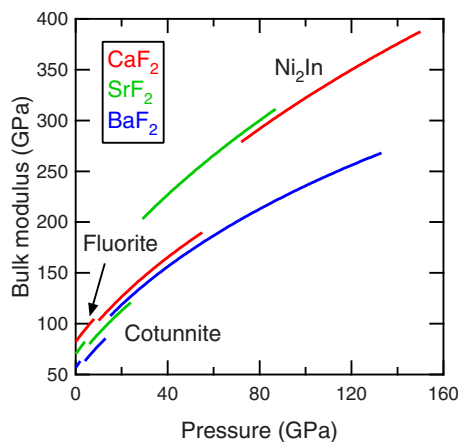


FIG. 8. (Color online) Bulk modulus vs pressure for  $\text{CaF}_2$ ,  $\text{SrF}_2$ , and  $\text{BaF}_2$  computed from Birch-Murnaghan equation of state fits to volume data. Gaps are left across phase transitions due to uncertainty in the compressibility in these regions.

## IV. DISCUSSION

### A. Static vs shock compression

$\text{CaF}_2$  and  $\text{BaF}_2$  have both been examined to above 250 GPa using shock compression techniques.<sup>37,58,63,64</sup> These studies have identified phase transitions under dynamic loading and determined the equation of state along the Hugoniot. For both  $\text{CaF}_2$  and  $\text{BaF}_2$ , x-ray examination of samples recovered from shock loading to 12–50 GPa showed partial transformation to the cotunnite-type phase.<sup>58</sup> The volume of the recovered cotunnite-type material was about 10% less than that of the fluorite phase, consistent with the static data reported in Table IV. In Fig. 11, Hugoniot data for  $\text{CaF}_2$  (Refs. 37 and 63) and  $\text{BaF}_2$  (Ref. 64) are plotted together with our and previous static measurements.<sup>4,12</sup> The shock data for  $\text{CaF}_2$  at pressures below 100 GPa are qualitatively consistent with the transformation to the cotunnite-type phase: due to thermal effects along the Hugoniot, shock states lie at higher pressure (for a given volume) compared with static data. Below 25 GPa, the  $\text{BaF}_2$  shock data similarly accord with the static data.

Above 100 GPa, the shock data suggest that  $\text{CaF}_2$  transforms to a highly incompressible phase.<sup>37</sup> It was proposed that this change in compressibility is associated with a transformation to a phase with 11-fold or 12-fold coordination.<sup>38,58</sup> The transition to the  $\text{Ni}_2\text{In}$ -type phase occurs in  $\text{CaF}_2$  at 72 GPa, which might be compatible with the shock data if the transition is kinetically delayed under dynamic loading. However, the comparison of our static compression data with the shock compression data (Fig. 11) shows that the  $\text{Ni}_2\text{In}$ -type phase is much more compressible than the observed shock compression data. Furthermore, the transition to the  $\text{Ni}_2\text{In}$ -type phase of  $\text{BaF}_2$  near 14 GPa does not appear to be associated with an incompressible phase in shock or static data. Thus, the highly incompressible behavior in  $\text{CaF}_2$  under shock loading cannot be linked with the

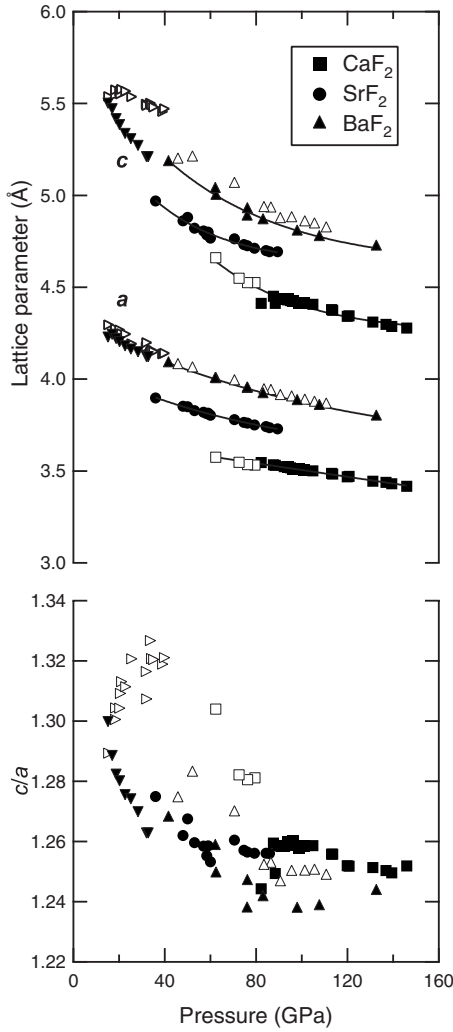


FIG. 9. Lattice parameters (upper panel) and  $c/a$  ratio (lower panel) for the  $\text{Ni}_2\text{In}$ -type phase of the alkaline earth fluorides. Filled symbols are for data under quasi-hydrostatic conditions while open symbols represent nonhydrostatic conditions. Open right-pointing triangles are from a nonhydrostatic experiment with a silicone grease medium (Ref. 16). Filled down-pointing triangles are from a hydrostatic experiment with a He medium (Ref. 12). In upper panel, least-squares fits are shown as a guide to the eye.

$\text{Ni}_2\text{In}$ -type phase, which does not have a notably high bulk modulus (Table V, Fig. 8).

The shock compression data for  $\text{BaF}_2$  (Ref. 64) do reveal similarly incompressible behavior above 100–150 GPa, the same or higher pressure than observed under shock loading in  $\text{CaF}_2$ . In our static experiments, we find no additional phase transitions in  $\text{CaF}_2$  or  $\text{BaF}_2$  in this pressure range to correspond with a highly incompressible phase, nor do we observe any additional high-temperature phases up to 3000 K. Whether additional phases appear in this system at the higher temperatures associated with shock loading is still unknown. The similarity of the pressures at which  $\text{CaF}_2$  and  $\text{BaF}_2$  become incompressible under shock loading suggest that, rather than a phase transition, thermal pressure may be responsible for the shock behavior of these compounds. Further shock compression studies of alkaline earth fluorides

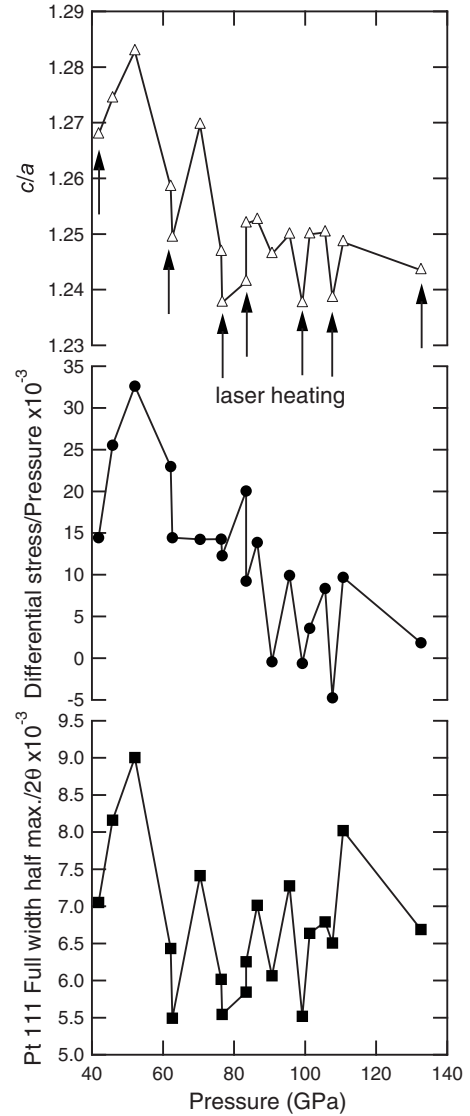


FIG. 10. For  $\text{BaF}_2$ , the  $c/a$  ratio of the  $\text{Ni}_2\text{In}$ -type phase (open triangles), the ratio of differential stress to pressure in Pt (filled circles), and the full width at half maximum for the Pt 111 peak normalized to the  $2\vartheta$  peak position (filled squares). The high degree of correlation ( $\rho=0.69$ ) between the  $c/a$  ratio and these indicators of differential stress explains the systematic difference between measurements of this phase in different pressure media. Under non-hydrostatic conditions, the  $c/a$  ratio of this phase increases while under quasi-hydrostatic conditions (after laser annealing at pressures indicated by arrows) it decreases.

above 1 Mbar are needed to better understand their dynamic response, and efforts should also be directed to identification of other high-pressure solid or liquid phases that may be responsible for the observed behavior.

## B. Phase-transition systematics

Figure 12 is a synthesis of the stable pressure ranges of known  $\text{AF}_2$  phases from this and other experimental and theoretical studies.<sup>5,16,65–71</sup> The fluoride system exhibits a remarkably systematic dependence of the structure on pressure

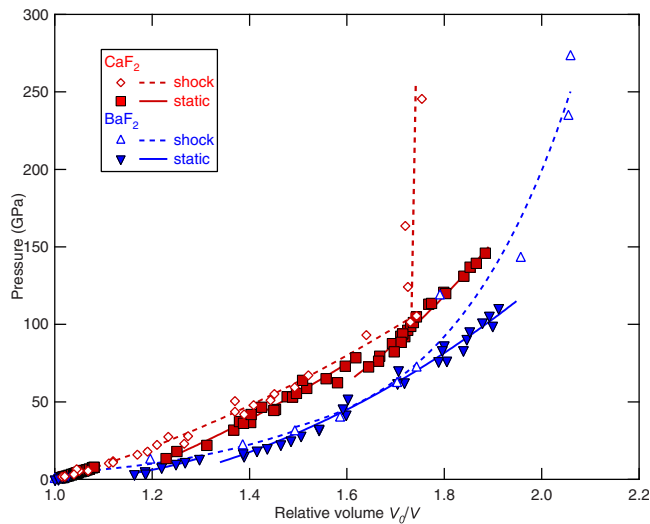


FIG. 11. (Color online) Shock compression data for  $\text{CaF}_2$  (Refs. 37 and 63) (open diamonds) and  $\text{BaF}_2$  (Ref. 64) (open up-pointing triangles) displayed with static data for  $\text{CaF}_2$  [filled squares, this study and Angel (Ref. 4)] and  $\text{BaF}_2$  [filled down-pointing triangles, this study and Smith *et al.* (Ref. 12)].

and atomic radius. This should be confirmed by further experimental study, particularly on  $\text{ZnF}_2$ ,  $\text{MnF}_2$ ,  $\text{PdF}_2$ , and  $\text{CdF}_2$ , none of which have been probed in the laboratory above 9 GPa.<sup>66–68</sup> The behavior of  $\text{PbF}_2$  deviates from the alkaline earth fluorides: although the  $\text{Ni}_2\text{In}$ -type phase has been predicted by theory,<sup>70</sup> experiments found instead an iso-

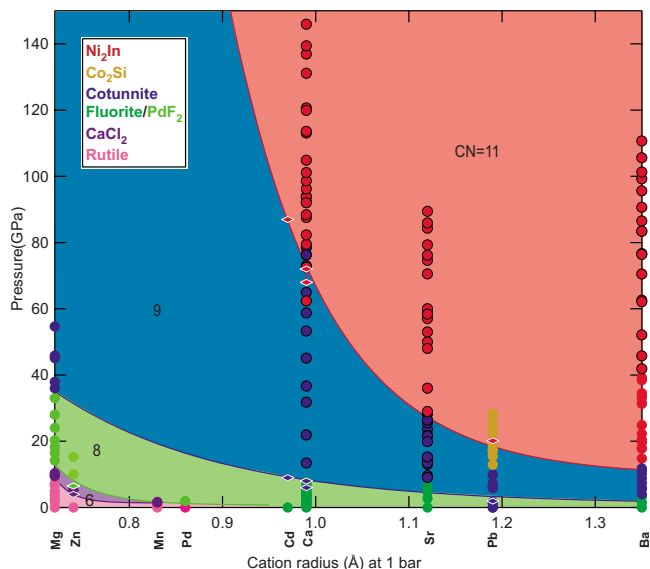


FIG. 12. (Color online) Phase stability range for fluoride compounds. Filled circles: experiment, diamonds: theory. Fluorite structures exhibit a systematic dependence on cation radius and pressure.  $\text{CaF}_2$ ,  $\text{SrF}_2$ , and  $\text{BaF}_2$  are constrained by this study (filled circles with black outlines). Other experimental data (filled circles without outlines) are from  $\text{PdF}_2$  (Ref. 68),  $\text{MnF}_2$  (Ref. 66),  $\text{BaF}_2$  (Ref. 16),  $\text{PbF}_2$  (Ref. 71),  $\text{MgF}_2$  (Ref. 69), and  $\text{ZnF}_2$  (Ref. 65). Transition pressures from theoretical calculations (diamonds) are shown for  $\text{PbF}_2$  (Ref. 70),  $\text{CaF}_2$  (Ref. 5),  $\text{CdF}_2$  (Ref. 67), and  $\text{ZnF}_2$  (Ref. 67).

symmetric transition to a  $\text{Co}_2\text{Si}$ -type structure.<sup>71</sup> This could possibly be due to the differences between the electronic structures of alkaline earth and transition-metal cations. As the evidence for an isosymmetric transition appears similar to the nonlinear compression behavior associated with the cotunnite- $\text{Ni}_2\text{In}$ -type transition, further work should be undertaken to confirm whether  $\text{Ni}_2\text{In}$ -type  $\text{PbF}_2$  can be synthesized.

A recent experiment<sup>72</sup> reported synthesis of an  $\text{AlB}_2$ -type phase with coordination number 12 in  $\text{BaH}_2$  at 50–65 GPa. This phase then is a plausible candidate for a higher-pressure polymorph in the fluoride system. Based on cation radius considerations,  $\text{BaF}_2$  would likely transform to this phase at the lowest pressure among fluorides. In addition, an insulator-metal transition<sup>8</sup> has also been predicted to occur in  $\text{BaF}_2$ . Recent theoretical calculations<sup>12</sup> predict the  $\text{AlB}_2$  phase would not be stable below 250 GPa and the insulator-metal transition would occur above 500 GPa. Our experimental study demonstrates that no further structural transformation in  $\text{BaF}_2$  occurs up to 133 GPa, and further experimental studies at ultrahigh pressures are necessary.

## V. SUMMARY

To explore the systematic variation in phase-transition pressures and compressibility of high-pressure phases as a function of cation size for the alkaline earth fluorides, we performed x-ray diffraction experiments on  $\text{CaF}_2$ ,  $\text{SrF}_2$ , and  $\text{BaF}_2$  in the diamond-anvil cell at pressures up to 146 GPa, 89 GPa, and 133 GPa, respectively. These compounds undergo a common sequence of structural transitions from fluorite to cotunnite at 9 GPa, 5 GPa, and 3 GPa, respectively, and from cotunnite to  $\text{Ni}_2\text{In}$ -type structure at 72 GPa, 29 GPa, and 14 GPa, respectively. For all three fluorides, the zero-pressure bulk modulus of the cotunnite-type phase is the same or slightly less than that of the fluorite phase. At the transition pressure, the bulk modulus of the  $\text{Ni}_2\text{In}$ -type phase is more strongly dependent on cation size. While for  $\text{BaF}_2$ , the transition to the  $\text{Ni}_2\text{In}$ -type phase results in a 10–20 % increase in bulk modulus, for  $\text{CaF}_2$  it increases the bulk modulus by 20–40 %. At 1 Mbar, the bulk moduli of the  $\text{Ni}_2\text{In}$ -type phases of  $\text{CaF}_2$ ,  $\text{SrF}_2$ , and  $\text{BaF}_2$  are 320 GPa, 330 GPa, and 240 GPa, respectively. Phase-transition pressures and bulk moduli for these high-pressure phases are within the wide range of theoretical predictions. Although the  $\text{Ni}_2\text{In}$ -type phase of  $\text{CaF}_2$  had been suggested by dynamic compression results to be a possible ultra-incompressible material, our data do not support this.

The  $\text{AF}_2$  system exhibits a systematic relationship between structure and cation/anion size ratio. Due to its large cation size and associated low phase-transition pressures,  $\text{BaF}_2$  had been the only compound in the  $\text{AF}_2$  system, demonstrated to transform to a  $\text{Ni}_2\text{In}$ -type phase. This work is an experimental confirmation of the  $\text{Ni}_2\text{In}$ -type structure in  $\text{CaF}_2$  and  $\text{SrF}_2$ .  $\text{AF}_2$  compounds with smaller cations than Ca, Sr, and Ba may undergo analogous cotunnite- $\text{Ni}_2\text{In}$ -type transitions at higher pressures than those explored in this work. The  $\text{Ni}_2\text{In}$ -type structure may also be a common post-cotunnite phase among other  $\text{AX}_2$  systems including materi-

als relevant to planetary science such as SiO<sub>2</sub> and possible superhard or super-incompressible materials such as TiO<sub>2</sub>. Because the compressibility of the Ni<sub>2</sub>In-type phase is more strongly dependent on cation than the cotunnite-type phase, further experimental work will be needed to determine the compressibility of Ni<sub>2</sub>In-type phases in other systems.

#### ACKNOWLEDGMENTS

We thank Q. Guo, S.-H. Shim, and K. Catali for experimental assistance and W. Nellis for helpful discussion. This work was supported by the NSF and the Carnegie-DOE Alliance Center. This work was performed at GeoSoilEnviroCARS (Sector 13) and High Pressure Collaborative Access

Team (HPCAT, Sector 16) at the Advanced Photon Source (APS), Argonne National Laboratory, and beamline X17B3, National Synchrotron Light Source (NSLS), Brookhaven National Laboratory. GeoSoilEnviroCARS is supported by the NSF, DOE, and the State of Illinois. HPCAT is supported by DOE-BES, DOE-NNSA, NSF, and the W.M. Keck Foundation. Use of the APS and NSLS was supported by the U.S. Department of Energy, Office of Basic Energy Sciences. X17B3 is supported by the NSF Cooperative Agreement No. EAR 01-35554 to COMPRES (CONsortium for Materials Properties Research in Earth Sciences). Use of the National Synchrotron Light Source, Brookhaven National Laboratory, was supported by the U.S.-DOE under Contract No. DE-AC02-10886.

\*Present address: Transnet Corporation.

†Present address: University of Texas, Austin.

‡Present address: Sumitomo Corporation.

- <sup>1</sup>J. M. Leger and J. Haines, *Eur. J. Solid State Inorg. Chem.* **34**, 785 (1997).
- <sup>2</sup>K. Kawano, T. Ohya, T. Tsurumi, K. Katoh, and R. Nakata, *Phys. Rev. B* **60**, 11984 (1999).
- <sup>3</sup>R. M. Hazen and L. W. Finger, *J. Appl. Crystallogr.* **14**, 234 (1981).
- <sup>4</sup>R. J. Angel, *J. Phys.: Condens. Matter* **5**, L141 (1993).
- <sup>5</sup>X. Wu, S. Qin, and Z. Wu, *Phys. Rev. B* **73**, 134103 (2006).
- <sup>6</sup>A.-m. Hao, X.-c. Yang, J. Li, W. Xin, S.-h. Zhang, X.-y. Zhang, and R.-p. Liu, *Chin. Phys. Lett.* **26**, 077103 (2009).
- <sup>7</sup>V. Kanchana, G. Vaitheeswaran, and M. Rajagopalan, *Physica B* **328**, 283 (2003).
- <sup>8</sup>V. Kanchana, G. Vaitheeswaran, and M. Rajagopalan, *J. Alloys Compd.* **359**, 66 (2003).
- <sup>9</sup>H. Jiang, R. Pandey, C. Darrigan, and M. Rérat, *J. Phys.: Condens. Matter* **15**, 709 (2003).
- <sup>10</sup>H. Shi, W. Luo, B. Johansson, and R. Ahuja, *J. Phys.: Condens. Matter* **21**, 415501 (2009).
- <sup>11</sup>S. Cui, W. Feng, H. Hu, Z. Feng, and Y. Wang, *Comput. Mater. Sci.* **47**, 41 (2009).
- <sup>12</sup>J. S. Smith, S. Desgreniers, J. S. Tse, J. Sun, D. D. Klug, and Y. Ohishi, *Phys. Rev. B* **79**, 134104 (2009).
- <sup>13</sup>Z.-y. Zeng, X.-r. Chen, J. Zhu, and C.-e Hu, *Chin. Phys. Lett.* **25**, 230 (2008).
- <sup>14</sup>A. Kavner, *Phys. Rev. B* **77**, 224102 (2008).
- <sup>15</sup>L. Gerward, J. Staun Olsen, S. Steenstrup, M. Malinowski, S. Asbrink, and A. Waskowska, *J. Appl. Crystallogr.* **25**, 578 (1992).
- <sup>16</sup>J. M. Leger, J. Haines, A. Atouf, O. Schulte, and S. Hull, *Phys. Rev. B* **52**, 13247 (1995).
- <sup>17</sup>E. Francisco, M. A. Blanco, and G. Sanjurjo, *Phys. Rev. B* **63**, 094107 (2001).
- <sup>18</sup>A. P. Ayala, *J. Phys.: Condens. Matter* **13**, 11741 (2001).
- <sup>19</sup>A. M. Pendás, J. M. Recio, M. Flórez, V. Luaña, and M. Bermejo, *Phys. Rev. B* **49**, 5858 (1994).
- <sup>20</sup>G. A. Samara, *Phys. Rev. B* **13**, 4529 (1976).
- <sup>21</sup>S. Alterovitz and D. Gerlich, *Phys. Rev. B* **1**, 2718 (1970).
- <sup>22</sup>S. Speziale and T. S. Duffy, *Phys. Chem. Miner.* **29**, 465 (2002).
- <sup>23</sup>C. Wong and D. E. Schuele, *J. Phys. Chem. Solids* **29**, 1309 (1968).
- <sup>24</sup>H. I. Smith and J. H. Chen, *Bull. Am. Phys. Soc.* **11**, 414 (1966).
- <sup>25</sup>D. P. Dandekar and J. C. Jamieson, *Trans. Am. Crystallogr. Assoc.* **5**, 19 (1969).
- <sup>26</sup>K.-F. Seifert, *Ber. Bunsenges. Phys. Chem* **70**, 1041 (1966).
- <sup>27</sup>G. A. Kourouklis and E. Anastassakis, *Phys. Rev. B* **34**, 1233 (1986).
- <sup>28</sup>L. S. Dubrovinsky, N. A. Dubrovinskaia, V. Swamy, J. Muscat, N. M. Harrison, R. Ahuja, B. Holm, and B. Johansson, *Nature (London)* **410**, 653 (2001).
- <sup>29</sup>N. A. Dubrovinskaia, L. S. Dubrovinsky, R. Ahuja, V. B. Prakapenka, V. Dmitriev, H.-P. Weber, J. M. Osorio-Guillen, and B. Johansson, *Phys. Rev. Lett.* **87**, 275501 (2001).
- <sup>30</sup>S. R. Shieh, A. Kubo, T. S. Duffy, V. B. Prakapenka, and G. Shen, *Phys. Rev. B* **73**, 014105 (2006).
- <sup>31</sup>J. Haines, J. M. Leger, and O. Schulte, *J. Phys.: Condens. Matter* **8**, 1631 (1996).
- <sup>32</sup>S. Desgreniers and K. Lagarec, *Phys. Rev. B* **59**, 8467 (1999).
- <sup>33</sup>O. Ohtaka, H. Fukui, T. Kunisada, T. Fujisawa, K. Funakoshi, W. Utsumi, T. Irifune, K. Kuroda, and T. Kikegawa, *Phys. Rev. B* **63**, 174108 (2001).
- <sup>34</sup>O. Ohtaka, H. Fukui, T. Kunisada, T. Fujisawa, K. Funakoshi, W. Utsumi, T. Irifune, K. Kuroda, and T. Kikegawa, *J. Am. Ceram. Soc.* **84**, 1369 (2001).
- <sup>35</sup>S. Duclos, Y. K. Vohra, A. L. Ruoff, A. Jayaraman, and G. P. Espinosa, *Phys. Rev. B* **38**, 7755 (1988).
- <sup>36</sup>A. R. Oganov, M. J. Gillan, and G. D. Price, *Phys. Rev. B* **71**, 064104 (2005).
- <sup>37</sup>L. V. Al'tshuler, M. A. Podurets, G. V. Simakov, and R. F. Trunin, *Sov. Phys. Solid State* **15**, 969 (1973).
- <sup>38</sup>W. J. Nellis and T. Petach, *Shock Compression of Condensed Matter-2007* (American Institute of Physics, New York, 2007), pp. 89–92.
- <sup>39</sup>H.-y. Chung, M. B. Weinberger, J. B. Levine, A. Kavner, J. M. Yang, S. H. Tolbert, and R. B. Kaner, *Science* **316**, 436 (2007).
- <sup>40</sup>R. Yu, Q. Zhan, and L. C. De Jonghe, *Angew. Chem., Int. Ed.* **46**, 1136 (2007).
- <sup>41</sup>R. Ahuja and L. S. Dubrovinsky, *High Press. Res.* **22**, 429 (2002).
- <sup>42</sup>Y. Al-Khatatbeh, K. K. M. Lee, and B. Kiefer, *Phys. Rev. B* **79**,

- 134114 (2009).
- <sup>43</sup>D. Nishio-Hamane, A. Shimizu, R. Ahuja, K. Niwa, A. Sano-Furukawa, T. Okada, T. Yagi, and T. Kikegawa, *Phys. Chem. Miner.* **37**, 129 (2010).
- <sup>44</sup>B. Kiefer and T. S. Duffy, *J. Appl. Phys.* **97**, 114902 (2005).
- <sup>45</sup>M. Rivers, V. Prakapenka, A. Kubo, C. Pullins, C. M. Holl, and S. D. Jacobsen, *High Press. Res.* **28**, 273 (2008).
- <sup>46</sup>Y. Meng, G. Shen, and H.-k. Mao, *J. Phys.: Condens. Matter* **18**, S1097 (2006).
- <sup>47</sup>V. B. Prakapenka, A. Kubo, A. Kuznetsov, A. Laskin, O. Shkurikhin, P. Dera, M. L. Rivers, and S. R. Sutton, *High Press. Res.* **28**, 225 (2008).
- <sup>48</sup>G. Shen, M. L. Rivers, Y. Wang, and S. R. Sutton, *Rev. Sci. Instrum.* **72**, 1273 (2001).
- <sup>49</sup>A. P. Hammersley, S. O. Svensson, M. Hanfland, A. N. Fitch, and D. Häusermann, *High Press. Res.* **14**, 235 (1996).
- <sup>50</sup>T. J. B. Holland and S. A. T. Redfern, *Miner. Mag.* **61**, 65 (1997).
- <sup>51</sup>A. C. Larson and R. B. Von Dreele, Los Alamos National Laboratory Report No. LAUR 86-748, 2000 (unpublished).
- <sup>52</sup>B. H. Toby, *J. Appl. Crystallogr.* **34**, 210 (2001).
- <sup>53</sup>N. C. Holmes, J. A. Moriarty, G. R. Gathers, and W. J. Nellis, *J. Appl. Phys.* **66**, 2962 (1989).
- <sup>54</sup>A. K. Singh, *J. Appl. Phys.* **73**, 4278 (1993).
- <sup>55</sup>S.-H. Shim, T. S. Duffy, and G. Shen, *Phys. Earth Planet. Inter.* **120**, 327 (2000).
- <sup>56</sup>E. Menéndez-Proupin and A. K. Singh, *Phys. Rev. B* **76**, 054117 (2007).
- <sup>57</sup>E. Morris, T. Groy, and K. Leinenweber, *J. Phys. Chem. Solids* **62**, 1117 (2001).
- <sup>58</sup>V. N. German, N. N. Orlova, M. N. Pavlovskii, L. A. Tarasova, and R. F. Trunin, *Izv. Acad. Sci. USSR, Phys. Solid Earth* **8**, 487 (1975).
- <sup>59</sup>T. S. Duffy, G. Shen, D. L. Heinz, J. Shu, Y. Ma, H.-k. Mao, R. J. Hemley, and A. K. Singh, *Phys. Rev. B* **60**, 15063 (1999).
- <sup>60</sup>R. J. Angel, M. Bujak, J. Zhao, G. D. Gatta, and S. D. Jacobsen, *J. Appl. Crystallogr.* **40**, 26 (2007).
- <sup>61</sup>K. Kunc, I. Loa, and K. Syassen, *Phys. Rev. B* **77**, 094110 (2008).
- <sup>62</sup>I. Jackson, *Geophys. J. Int.* **134**, 291 (1998).
- <sup>63</sup>M. Hasegawa, K. Kondo, and A. Sawaoka, *Jpn. J. Appl. Phys., Part 1* **23**, 20 (1984).
- <sup>64</sup>R. F. Trunin, L. F. Gudarenko, M. V. Zhernokletov, and G. V. Simakov, *Experimental Data on Shock Compressibility and Adiabatic Expansion of Condensed Substances* (RFNC-VNIIEF, Sarov, Russia, 2001).
- <sup>65</sup>K. Kusaba and T. Kikegawa, *Solid State Commun.* **145**, 279 (2008).
- <sup>66</sup>M. Yamaguchi, T. Yagi, N. Hamaya, and T. Yagi, *J. Phys. Soc. Jpn.* **61**, 3883 (1992).
- <sup>67</sup>X. Wu and Z. Wu, *Eur. Phys. J. B* **50**, 521 (2006).
- <sup>68</sup>A. Tressaud, J. L. Soubeyroux, H. Touhara, G. Demazeau, and F. Langlais, *Mater. Res. Bull.* **16**, 207 (1981).
- <sup>69</sup>J. Haines, J. M. Leger, F. Gorelli, D. D. Klug, J. S. Tse, and Z. Q. Li, *Phys. Rev. B* **64**, 134110 (2001).
- <sup>70</sup>A. Costales, M. A. Blanco, R. Pandey, and J. M. Recio, *Phys. Rev. B* **61**, 11359 (2000).
- <sup>71</sup>J. Haines, J. M. Leger, and O. Schulte, *Phys. Rev. B* **57**, 7551 (1998).
- <sup>72</sup>K. Kinoshita, M. Nishimura, Y. Akihama, and H. Kawamura, *Solid State Commun.* **141**, 69 (2007).